Molecular Aspects

NaCl triggers the CRP-dependent increase of cAMP in *Mycobacterium tuberculosis*

Sonia Rebollo-Ramirez, Gerald Larrouy-Maumus[*]

MRC Centre for Molecular Bacteriology and Infection, Department of Life Sciences, Faculty of Natural Sciences, Imperial College London, London, UK

ARTICLE INFO

ABSTRACT

The second messenger 3′,5′-cyclic adenosine monophosphate (3′,5′-cAMP) has been shown to be involved in the regulation of many biological processes ranging from carbon catabolite repression in bacteria to cell signalling in eukaryotes. In mycobacteria, the role of cAMP and the mechanisms utilized by the bacterium to adapt to and resist immune and pharmacological sterilization remain poorly understood. Among the stresses encountered by bacteria, ionic and non-ionic osmotic stresses are among the best studied. However, in mycobacteria, the link between ionic osmotic stress, particularly sodium chloride, and cAMP have been relatively unexplored. Using a targeted metabolic analysis combined with stable isotope tracing, we show that the pathogenic *Mycobacterium tuberculosis* but not the opportunistic pathogen *Mycobacterium marinum* nor the non-pathogenic *Mycobacterium smegmatis* responds to NaCl stress via an increase in intracellular cAMP levels. We further showed that this increase in cAMP is dependent on the cAMP receptor protein and in part on the threonine/serine kinase PknD, which has previously been associated with the NaCl stress response in mycobacteria.

1. Introduction

The ability to sense and respond to a changing environment is essential for all organisms, and appropriate responses are coordinated through signal transduction systems. Cyclic mono- and di-nucleotides, (p)ppGpp, Ca^{2+}, inositol phosphate, and diacylglycerol function as second messengers in many organisms [1–3]. 3′,5′-Cyclic adenosine monophosphate (cAMP), one of the most widely used second messengers and a key modulator of bacterial physiology, regulates a variety of cellular processes ranging from carbon metabolism to virulence [4,5]. Ionic or electrolyte stress and non-ionic or non-electrolyte osmotic stress, mediated by sodium chloride (NaCl) and sucrose or glucose, respectively, are examples of many environmental hazards encountered by bacteria, but our understanding of how bacteria perceive and respond to changes in extracellular osmolarity is incomplete. In the model organism *E. coli*, the level of cAMP is a key factor in osmoregulation via the cAMP receptor protein (CRP) [6–8].

The genus *Mycobacterium* encompasses over 100 species, including pathogenic mycobacteria such as *Mycobacterium tuberculosis* (Mtb), responsible for human tuberculosis (TB); opportunistic or non-tuberculous mycobacteria (NTM), which include *Mycobacterium avium* and *Mycobacterium kansasii*; and non-pathogenic mycobacteria such as *Mycobacterium smegmatis*. In mycobacteria, cAMP signalling is important for metabolism, such as propionate acquisition via the cAMP-dependent lysine acetyltransferase, virulence and host cell interactions [9–11]. Previous work has shown that the concentration of cAMP in macrophages increases by up to 4-fold upon infection with Mtb and *M. microti* and that intracellular levels of cAMP increase by up to 50-fold in Mtb and *M. bovis* BCG [12,13], leading to cAMP intoxication in the host cells [9]. This second messenger is known to influence several important aspects of the cellular response to infection [13]. These aspects include the production of TNF-α via the protein kinase A and cAMP-response-element-binding (CREB) protein pathway [9], as well as modulation of phagosome trafficking via inhibition of phagosome-lysosome fusion [14–16]. Moreover, in *M. smegmatis*, cAMP has been proposed to modulate fatty acid synthesis [17,18]. These observations highlight a critical role for cAMP in host colonization by Mtb [9,12]. Several publications have reported elevated cAMP levels under other stress conditions, such as SDS-mediated cell-envelope stress and nitric oxide, hydrogen peroxide and heat stress [19,20]. For example, cAMP levels are 2-fold elevated in Mtb following heat stress, whereas other stress conditions such as oxidative, nitrosative or low pH do not affect the intracellular cAMP pool *in vitro* [20]. Similarly, Dass et al. reported a more than 300-fold increase in cAMP levels when *M. smegmatis* was exposed to 0.5% SDS over a period of 1.5 h [19]. However, the effect of ionic osmotic stress, such as that induced by NaCl, which is an

electrolyte ubiquitously found within the host, on cAMP levels has not yet been investigated in mycobacteria. Throughout their life cycle, mycobacteria survive in a variety of adverse conditions and concentrations of sodium chloride [21–24]. It is well established that mycobacteria respond to ionic and non-ionic osmotic stress via an increase in common solutes such as glycerol and trehalose and have a two-step adaptation model: a fast metabolic response independent of a late response-involving lipid remodelling [23]. In addition, Hatzios et al. proposed that PknD, a eukaryotic-like serine/threonine protein kinase, is the primary protein involved in the osmosensory pathway of Mtb [22].

Therefore, in this study, we investigated whether mycobacteria respond to a physiological concentration of NaCl, 250 mM [21], via modulation of their intracellular cAMP levels. This evaluation was performed by using a combination of LC-MS-based metabolite analysis, stable isotope labelling, and genetic mutants. These analyses revealed that the pathogenic mycobacteria Mtb responds to NaCl stress via an increase in the intracellular cAMP pool size. We found that even if the increase in intracellular cAMP levels is partly mediated by PknD, it is the transcriptional regulator cAMP receptor protein (CRP, Rv3676) that orchestrates the overall process.

2. Material and methods

2.1. Materials

Unless otherwise stated, all chemicals and reagents were purchased from Sigma-Aldrich.

2.1.1. Bacterial strains and growth conditions

M. tuberculosis H37Rv (Mtb), *M. tuberculosis* CDC1551, *M. smegmatis* mc^{2}155 and *M. marinum* M were used in this study. Mycobacteria were cultured up to mid-exponential phase in 7H9 liquid medium supplemented with 0.5 g/l Fraction V bovine serum albumin, 0.05% tyloxapol, 0.2% dextrose, 0.2% glycerol, and 10 mM NaCl. For metabolomic profiling studies, mycobacteria were cultured on 7H10 agar supplemented with 0.5 g/l Fraction V bovine serum albumin, 0.2% dextrose, 0.2% glycerol and 10 mM NaCl. Throughout the study, mycobacteria were cultured in a shaking incubator set at 125 rpm and 37 °C for all Mtb strains and *M. smegmatis*; for *M. marinum* M, the optimal growth temperature was set at 30 °C. The Mtb strain CDC1551 and its isogenic transposon mutant strain *rv0516::Tn* were obtained from the Tuberculosis Animal Research and Gene Evaluation Taskforce (National Institutes of Health/National Institute of Allergy and Infectious Diseases contract no. N01 AI-30036). The *M. tuberculosis* H37Rv (Mtb), *M. smegmatis* mc^{2}155 and *M. marinum* M were from the laboratory strains collection at Imperial College London, UK. The *M. tuberculosis* H37Rv parental, knockout for Rv3676 (CRP) and complemented strains were provided by Dr Roger Buxton MRC-National Institute for Medical Research [25].

2.1.2. Bacteria viability

Bacteria were gown to early log phase (OD ~0.2) and exposed to 10 mM NaCl, 250 mM NaCl or 500 mM sucrose for ¼ and 1 or 2 doubling times. Colony-forming units per millilitre (CFU/ml) were determined by performing serial 10-fold dilutions in 96-well plates using culture medium Middlebrook 7H9 broth. Twenty microlitres of each dilution was loaded and spread onto the Middlebrook 7H10 agar and incubated at an appropriate temperature (see the Bacterial strains and growth conditions section) until the formation of CFU, typically 4 days for *M. smegmatis*, 3 weeks for *M. marinum* and 3–5 weeks for *M. tuberculosis* strains.

2.1.3. Metabolite extraction experiments

For targeted metabolomic profiling studies, mycobacteria were cultured as described previously [23,26–28]. Briefly, mycobacteria

were grown initially in 7H9 liquid medium containing the carbon sources of interest until the OD_{600} reached ~0.8–1. Bacteria were then inoculated onto 0.22 μm nitrocellulose filters under vacuum filtration. Mycobacterial-laden filters were then placed on top of chemically equivalent agar media (described above) and allowed to grow at 37 °C or 30 °C for 5 doubling times to generate enough biomass for targeted metabolomics studies. Filters were then transferred into 7H10 plates supplemented with 0.5 g/l fraction V bovine serum albumin, 0.2% dextrose and 0.2% glycerol containing either 10 mM NaCl, 250 mM NaCl or 500 mM sucrose. Bacteria were metabolically quenched by plunging the filters into the extraction solution composed of acetonitrile/methanol/H$_2$O (2:2:1) pre-cooled to −40 °C. Small molecules were extracted by mechanical lysis of the entire bacteria-containing solution with 0.1 mm acid-washed zirconia beads for 1 min using a FastPrep (MPBio®) set at 6.0 m/s. Lysates were filtered through 0.22 μm Spin-X column filters (Costar®). Bacterial biomass of individual samples was determined by measuring the residual protein content of the metabolite extracts using the BCA assay kit (Thermo®) [29,30].

2.1.4. Liquid-chromatography-mass spectrometry

Metabolomics-Aqueous normal phase liquid chromatography was performed using an Agilent 1290 Infinity II LC system equipped with a binary pump, temperature-controlled auto-sampler (set at 4 °C) and temperature-controlled column compartment (set at 25 °C) containing a Cogent Diamond Hydride Type C silica column (150 mm × 2.1 mm; dead volume 315 μl). A flow rate of 0.4 ml/min was used. Elution of polar metabolites was carried out using solvent A consisting of deionized water (resistivity ~18 MΩ cm) and 0.2% acetic acid and solvent B consisting of 0.2% acetic acid in acetonitrile. The following gradient was used: 0 min 85% B; 0–2 min 85% B; 3–5 min to 80% B; 6–7 min 75% B; 8–9 min 70% B; 10–11 min 50% B; 11.1–14 min 20% B; 14.1–25 min hold 20% B followed by a 5 min re-equilibration period at 85% B at a flow rate of 0.4 ml/min. Accurate mass spectrometry was carried out using an Agilent Accurate Mass 6545 QTOF apparatus. Dynamic mass axis calibration was achieved by continuous infusion, post-chromatography, of a reference mass solution using an isocratic pump connected to an ESI ionization source operated in the positive-ion mode. The nozzle voltage and fragmentor voltage were set at 2000 V and 100 V, respectively. The nebulizer pressure was set at 50 psig, and the nitrogen drying gas flow rate was set at 5 l/min. The drying gas temperature was maintained at 300 °C. The MS acquisition rate was 1.5 spectra/sec, and *m/z* data ranging from 50–1200 were stored. This instrument enabled accurate mass spectral measurements with an error of less than 5 parts-per-million (ppm), mass resolution ranging from 10,000–45,000 over the *m/z* range of 121–955 atomic mass units, and a 100,000-fold dynamic range with picomolar sensitivity. The data were collected in the centroid 4 GHz (extended dynamic range) mode. Detected *m/z* were deemed to be identified metabolites on the basis of unique accurate mass-retention time and MS/MS fragmentation identifiers for masses exhibiting the expected distribution of accompanying isotopomers. Typical variation in abundance for most of the metabolites remained between 5 and 10% under these experimental conditions.

2.1.5. ^{13}C-labelling analysis

Under the experimental conditions described above using [U-$^{13}C_3$] glycerol (99%) and [U-$^{13}C_6$] glucose (99%), the extent of ^{13}C labelling for each metabolite was determined by dividing the summed peak height ion intensities of all ^{13}C-labelled species by the ion intensity of both labelled and unlabelled species using the software Agilent Profinder version B.8.0.00 service pack 3.

2.1.6. cAMP standard curve

3′,5′-cAMP and 2′,3′-cAMP were used at 100 mM stock solution is double-distilled water and serial diluted, in a solution composed of acetonitrile/methanol/H$_2$O (2:2:1), from 1 mM down to 0.1 nM in technical quadruplicate. Standard curve was established using Agilent

Quantitative Analysis B.07.00.

2.1.7. Transcriptomics

M. tuberculosis H37Rv parental strain was grown in 7H9 liquid medium at 37 °C containing 10 mM NaCl as described above. Bacteria were stressed by the addition of NaCl to a concentration of 250 mM NaCl after 1/12, 1/3 and 1 doubling times at mid-log phase (light transmittance at 600 nm–0.6). Total RNA was extracted using a fast RNA pro bluekit (MP Biomedicals). RNA was treated with RNase-free DNase (Promega) and purified using RNAeasy columns (Qiagen) according to the manufacturer's instructions. Fluorescently labelled cDNA was generated from total RNA (1 μg) by direct incorporation of Cy3- or Cy5-dCTP (GE Healthcare) using Superscript III Reverse Transcriptase (Invitrogen Life Technologies) in the presence of random hexamers (3 μg), dNTPs (185 μM dCTP and 463 μM each of dATP, dGTP and dTTP) and Cy3-dCTP or Cy5-dCTP (1.7 nmoles). RNA and random hexamers were initially mixed, made up to a volume of 11 μl and heated to 95 °C for 5 min. The mixture was then chilled on ice for 2 min. Remaining components of the reverse transcriptase reaction were added, and the mixture was incubated for 10 min at 25 °C, followed by 42 °C for 90 min. Samples to be compared were mixed, and the labelled cDNA was purified using MinElute PCR purification columns (Qiagen). *M. tuberculosis* whole-genome microarray slides (prepared at St. George's, University of London) were initially prehybridized in 3.5 × SSC, 0.1% SDS and 10 mg/ml BSA for 20 min at 65 °C and then washed with deionized water and isopropanol. Labelled samples were heated for 2 min at 95 °C in 4xSSC and 0.3% SDS and hybridized on microarray slides under lifter slips (Thermo Scientific) for 16–20 h at 65 °C in a dark hybridization chamber. Hybridized slides were washed once with 1xSSC, 0.05% SDS at 65 °C and then twice with 0.06xSSC at room temperature. Washed slides were dried by centrifugation and scanned for fluorescence with a GenePix 4000B microarray scanner. Grids were fitted to the raw microarray images, and background normalization and spot quantitation were performed using Bluefuse software (BlueGnome Ltd., Cambridge, United Kingdom); normalized readings were plotted using GeneSpring 10 software (Silicon Genetics). Data were obtained for six slides, including dye swaps, from three bacterial cultures. Data were initially filtered according to expression, and the lower 20th percentile was eliminated from the analysis. Genes that showed > 2-fold change in absolute expression with a p-value < 0.05 (Student's t-test) were considered to be altered.

2.1.8. Statistical analysis

For power calculation, data are presented as the mean ± standard error of the mean from 2 biological replicates and 3 technical replicates per condition. Unpaired two-tailed Student's *t*-tests were used to compare values, with p < 0.05 considered significant. Fold changes in intracellular cAMP levels were expressed as a ratio (NaCl-challenged bacteria/untreated bacteria) at each corresponding time point as described in the figures and figure legends. The standard deviations were calculated according to the error propagation in calculated ratios [31].

2.1.9. Biological safety considerations

Bacteria were handled within a Class-I or Class-II safety-level cabinet equipped with UV light source and HEPA filters.

3. Results and discussion

In this study, we focused on the intracellular cAMP levels in non-pathogenic, opportunistic and pathogenic mycobacteria grown in conventional 7H9 culture medium containing either 10 mM, considered the control, or 250 mM NaCl, which is equivalent to the concentration that has been reported in macrophages [21,23]. Unlike *E. coli*, *Corynebacterium glutamicum* and *Streptomyces coelicolor,* which possess only one adenylate cyclase (AC), mycobacteria possess several copies of ACs in their genome and are known to produce and secrete large amounts of

cAMP during growth compared to those produced by other bacteria [19,32]. Sixteen genes are found in the Mtb H37Rv genome encoding for class III AC, 8 genes in *M. smegmatis*, 12 genes in *M. avium* and 31 genes in *M. marinum* [33,34]. In parallel, it is known that secretion of cAMP can subvert host cell metabolism [9], and *M. microti*, a member of the Mtb complex, blocks phagosome maturation by inducing cAMP production within macrophages [12]. It is well established that intracellular cAMP mediates its regulatory effects through allosteric interactions with cAMP-binding proteins, which undergo conformational changes altering their activity. Those modifications lead to global physiology remodelling. The Mtb H37Rv genome reveals ten putative proteins harbouring a cAMP-binding domain [35]. Among those proteins are two transcriptional regulators, which are crucial for virulence (CRP, Rv3676 and Cmr, Rv1675) [25,36,37]. Of the other cAMP-binding proteins, only the cAMP-dependent protein lysine acetyltransferase, crucial for carbon acquisition in *M. bovis* BCG, has been characterized [11,38,39]. Due to the importance of intracellular cAMP in mycobacterial physiology, we investigated whether the intracellular cAMP levels are altered upon NaCl stress in mycobacteria.

3.1. A physiological concentration of NaCl leads to an increase in intracellular cAMP levels in Mycobacterium tuberculosis

To investigate whether mycobacteria respond to different levels of ionic and non-ionic osmotic stress via a modulation of their intracellular cAMP levels similar to the response observed in *E. coli* [6], three different mycobacterial species were exposed to 10 mM NaCl, 250 mM NaCl and 500 mM sucrose. We chose *M. smegmatis* mc^{2}155 as a non-pathogenic mycobacteria, *M. marinum* M as an opportunistic mycobacteria, and the pathogenic Mtb H37Rv. A concentration of 500 mM sucrose was used as a control of non-ionic osmotic stress, which corresponds to ∼500 mOsm/l and is equivalent to the osmolarity of 250 mM NaCl [21]. We first monitored bacterial growth under those three conditions. As seen in Fig. 1, compared to the control condition, where bacteria where grown at a concentration of 10 mM NaCl, the presence of 250 mM NaCl reduces but does not abolish the growth of all three bacterial species, which is in accordance with the literature [23]. However, even if the growth of *M. smegmatis* is slightly impaired in the presence of 500 mM sucrose compared to 250 mM NaCl (Fig. 1A), this high concentration of sucrose drastically impaired the growth of *M. marinum* and Mtb (Fig. 1B and C). These observations were further confirmed by performing stress assays and monitoring the CFU/ml in those strains (Supplementary Fig. 1). This observation suggests that *M. smegmatis* is therefore more tolerant to non-ionic osmotic stress than *M. marinum* and Mtb. To investigate the correlation between the type of osmotic stress and the intracellular cAMP levels based on the growth curves, the bacteria were exposed for 1 doubling time to 10 mM NaCl, 250 mM NaCl and 500 mM sucrose (Fig. 1D, Table 1), and their intercellular cAMP levels were measured. Compared to unchallenged bacteria, *M. smegmatis* bacteria exposed to 250 mM NaCl and 500 mM sucrose showed a 1.65-fold and 4-fold decrease in intracellular cAMP levels. In *M. marinum*, although exposure to 500 mM sucrose led to a 4.5-fold decrease in intracellular cAMP levels, no changes were observed in the presence of 250 mM NaCl. In *M. smegmatis*, this observation is consistent with the classic model of NaCl stress response described in *E. coli,* where intracellular cAMP levels decrease with increasing concentrations of NaCl [6]. In contrast, even if the exposure to 500 mM sucrose led to a 1.5-fold decrease in intracellular cAMP levels in Mtb H37Rv, a 3-fold increase in the intracellular cAMP levels was observed upon exposure to a concentration of 250 mM NaCl for 1 doubling time (Fig. 1D). Thus far, the only organisms reported to respond to NaCl stress by an increase in intracellular cAMP levels are the soil amoeba *Dictyostelium discoideum* and the cyanobacterium *Anabaena* PCC 7120 [40,41]. At this stage, we confirmed the assignment of this molecule as the second messenger 3′,5′-cAMP. To do so, we used state-of-the-art LC-MS/MS (Fig. 2 and Supplementary Fig. S1). Under our
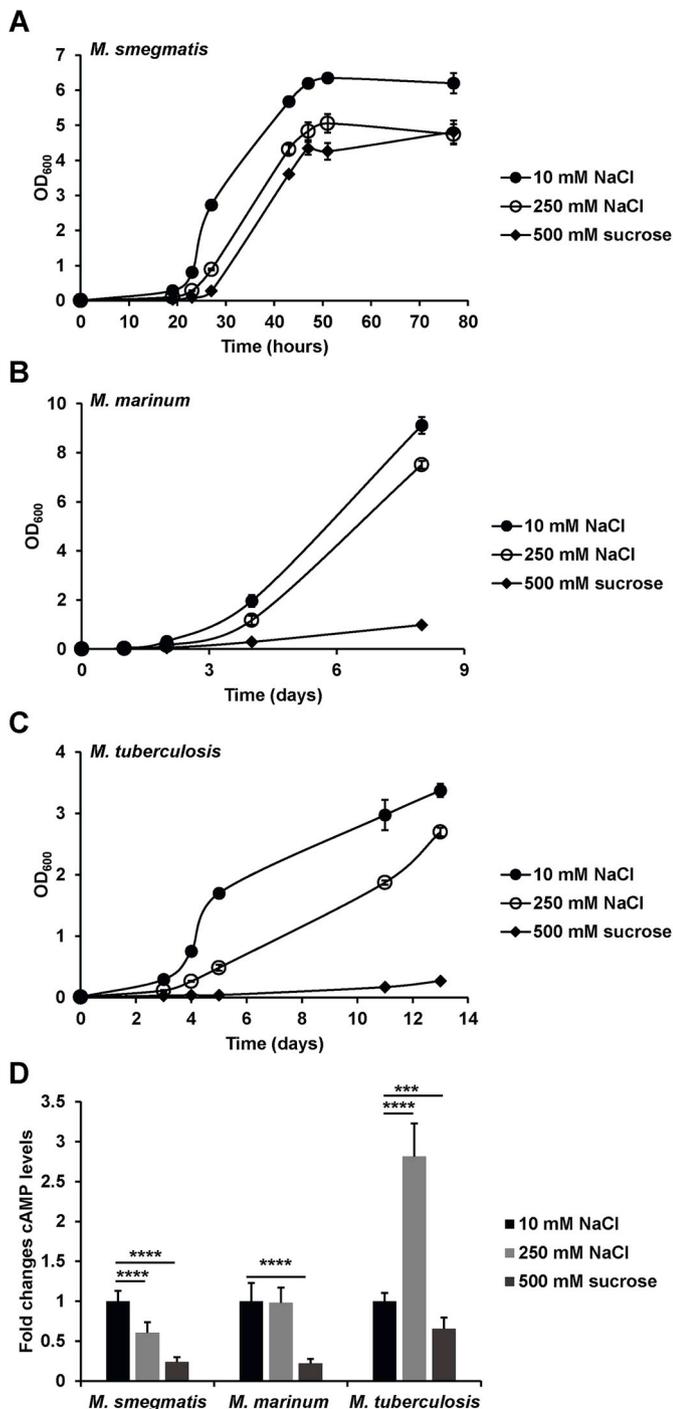
Fig. 1. Effect of ionic and non-ionic osmotic stresses on the growth and intracellular cAMP levels of *M. smegmatis* mc²155, *M. marinum* M and *M. tuberculosis* H37Rv. Growth curves at 10 mM NaCl (filled circle), 250 mM NaCl (open circle) and 500 mM sucrose (filled diamond) in Middlebrook 7H9 medium monitored at OD 600 nm for *M. smegmatis* (A), *M. marinum* (B) and *M. tuberculosis* (C). (D) Bar graph showing the intracellular levels of cAMP at 10 mM NaCl (black), 250 mM NaCl (light grey) and 500 mM sucrose (grey) for the equivalent of one doubling time for *M. smegmatis* mc²155, *M. marinum* M, and *M. tuberculosis* H37Rv. Data are the average of two biological replicates and three technical replicates. Data are presented as fold changes corresponding to the ratio of cAMP levels at 250 mM NaCl or 500 mM sucrose over cAMP levels at 10 mM NaCl of the corresponding time point. ***p < 0.001, ****p < 0.0001 as analysed by Student's *t*-test.

Table 1
Amount of cAMP in pmoles/100 μg protein for the strains used in this study.

Strains	Conditions	Time of exposure to stress (doubling time)	pmoles cAMP/ 100 μg protein
M. smegmatis mc²155	10 mM NaCl	1	12.4 ± 1.1
	250 mM NaCl	1	7.5 ± 1.5
	500 mM sucrose	1	3.0 ± 0.7
M. marinum M	10 mM NaCl	1	1.6 ± 0.3
	250 mM NaCl	1	1.5 ± 0.2
	500 mM sucrose	1	0.3 ± 0.1
M. tuberculosis H37Rv	10 mM NaCl	1	11.0 ± 0.8
	250 mM NaCl	1	31.0 ± 4.0
	500 mM sucrose	1	7.2 ± 1.5
M. tuberculosis CDC1551	10 mM NaCl	0	10.4 ± 1.7
		0.25	17.8 ± 2.4
		1	17.7 ± 1.5
	250 mM NaCl	0.25	64.4 ± 6.8
		1	33.5 ± 4.3
M. tuberculosis CDC1551 PknD::Tn	10 mM NaCl	0	0.9 ± 0.1
		0.25	1.7 ± 0.4
		1	1.6 ± 0.4
	250 mM NaCl	0.25	3.6 ± 0.7
		1	3.7 ± 0.5
M. tuberculosis H37Rv	10 mM NaCl	0	1.6 ± 0.3
		0.25	5.6 ± 0.4
		1	7.3 ± 0.7
	250 mM NaCl	0.25	31.6 ± 1.8
		1	17.6 ± 2.9
M. tuberculosis Δ*rv3676*	10 mM NaCl	0	2.2 ± 0.6
		0.25	2.8 ± 0.3
		1	3.3 ± 0.9
	250 mM NaCl	0.25	3.9 ± 0.1
		1	2.0 ± 0.7
M. tuberculosis comp. *rv3676*	10 mM NaCl	0	1.8 ± 0.3
		0.25	6.5 ± 0.3
		1	3.1 ± 0.6
	250 mM NaCl	0.25	10.3 ± 1.6
		1	29.5 ± 2.5

chromatographic conditions, the extract ion chromatogram of the standard 2′,3′-cAMP, which derives from mRNA degradation [42], has a retention time of 2.8 min (Fig. 2A) and the extract ion chromatogram of the standard 3′,5′-cAMP has a retention time of 3.6 min (Fig. 2B). The extract ion chromatograms for the molecule at *m/z* 330.0598 [M + H] + corresponding to cAMP in Mtb exposed to 10 mM for 1 doubling time and 250 mM for 1 doubling time are shown in Fig. 2C and D, respectively. As seen in Fig. 2C, both 2′,3′-cAMP and 3′,5′-cAMP can be detected and separated in Mtb metabolome extracts. In this extract, the second messenger, with a retention time of 3.6 min, represents the majority of the total pool of cAMP. Compared to unchallenged cells, the cells exposed to 250 mM NaCl exhibited an increase in only the peak at 3.6 min, assigned to 3′,5′-cAMP. This assignment was further confirmed using MS/MS (Supplementary Fig. 2), demonstrating that upon exposure to 250 mM NaCl, the intracellular 3′,5′-cAMP levels increased in Mtb.

3.2. cAMP is synthesised de novo upon NaCl stress

cAMP is synthesised from ATP via the action of adenylate cyclases. Therefore, the increase in cAMP observed upon exposure to a concentration of 250 mM NaCl can result either in the use of an existing ATP pool, or *de novo* ATP and cAMP synthesis. This suggests that cAMP is made on demand according to the magnitude of the stress sensed. The fact that we did not observe increases in intracellular levels of cAMP in *M. smegmatis* and *M. marinum* upon equivalent exposure to 250 mM
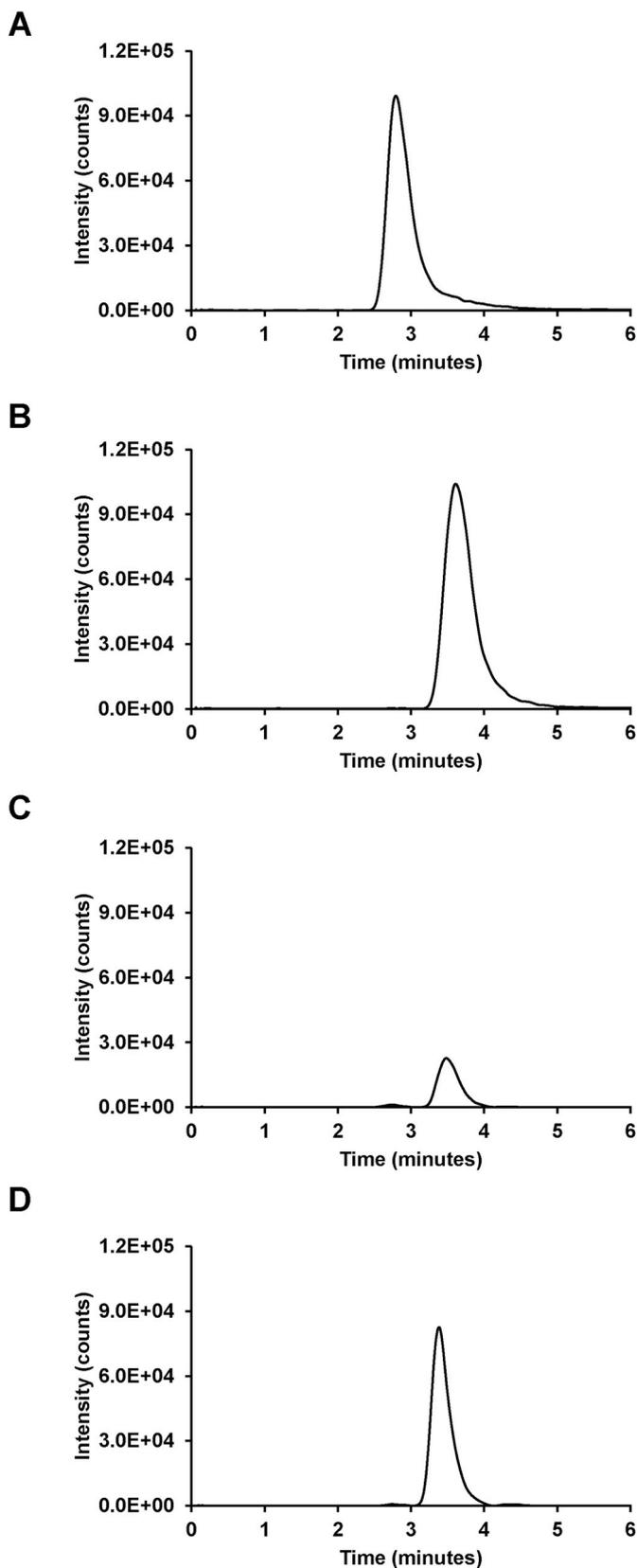
A

B

C

D

Fig. 2. Confirmation of the assignment of the molecule of interest as 3′,5′-cyclic adenosine monophosphate. (A) Extract ion chromatogram for the molecule at m/z 330.0598 in positive-ion mode $[M+H]+$ corresponding to 1 μM of the standard 2′,3′-cAMP. (B) Extract ion chromatogram for the molecule at m/z 330.0598 in positive-ion mode $[M+H]+$ corresponding to 1 μM of the standard 3′,5′-cAMP. (C) Extract ion chromatogram for the molecule at m/z 330.0598 in positive-ion mode $[M+H]^+$ after 1 doubling time exposure to 10 mM NaCl in *M. tuberculosis* H37Rv. (D) Extract ion chromatogram for the molecule at m/z 330.0598 in positive-ion mode $[M+H]^+$ after 1 doubling time exposure to 250 mM NaCl in *M. tuberculosis* H37Rv.
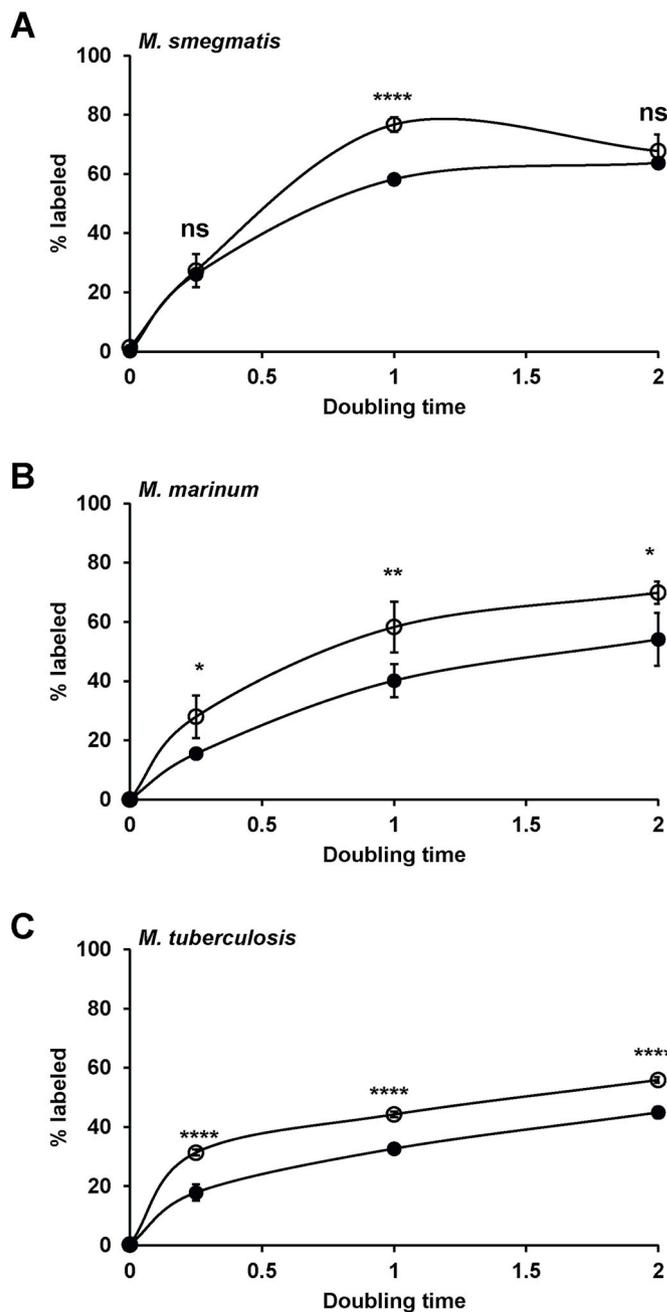
A

B

C

Fig. 3. Percentage of ^{13}C incorporation in cAMP over time at 10 mM NaCl (filled circle) and 250 mM NaCl (open circle) in *M. smegmatis* mc^{2}155 (A), *M. marinum* M (B) and *M. tuberculosis* H37Rv (C). Data are the average of two biological replicates and three technical replicates. *p < 0.05, **p < 0.01 ***p < 0.001, ****p < 0.0001 as analysed by Student's *t*-test.

NaCl could be due to a lack of expression of the adenylate cyclases in these organisms compared to Mtb under similar conditions of growth and stress. However, according to the literature, those enzymes are expressed under conventional growth conditions, precluding a lack of

expression under the conditions tested in this study [25,33,43–46]. Alternatively, another potential hypothesis is that the adenylate cyclases are expressed in those organisms but that a concentration of 250 mM NaCl is not able to alter their activity. Therefore, to enable an in-depth investigation into the synthesis and the turn-over of cAMP under the conditions used in this study, we chose to perform stable isotope tracing experiments at 10 mM and 250 mM NaCl in all three mycobacterial species. The bacteria were stressed in a culture medium supplemented with either 10 mM or 250 mM NaCl in the presence of [U-^{13}C$_3$] glycerol and [U-^{13}C$_6$] glucose. If cAMP was produced from the existing ATP pool, no changes in labelling of cAMP would be expected. However, if cAMP was produced following *de novo* ATP synthesis, the percentage of cAMP labelled would increase over time, which would be consistent with the increase in cAMP turn-over. If the adenylate cyclases were neither expressed nor active under the conditions used in this study, no ^{13}C incorporation in cAMP would be observed; in contrast, if the adenylate cyclases were expressed and active, we would expect to observe an increase in ^{13}C incorporation in cAMP over time in both conditions tested here. Fig. 3 represents the percentage of labelled cAMP over time in *M. smegmatis* at 1/3, 1 and 2 doubling times (Fig. 3A) and in *M. marinum* and Mtb at ¼, 1 and 2 doubling times (Fig. 3B and C, respectively) exposed to 10 mM and 250 mM NaCl. As seen in Fig. 3, at 10 mM NaCl, all strains used in this study exhibited an increase in the percentage of cAMP labelled over time, ruling out non-expression or a lack of activity of the adenylate cyclases in those species; this finding is consistent with the literature and indicates cAMP turn-over in all the mycobacterial species used here [25,43–45]. After 2 doubling times at 10 mM NaCl, the percentage of labelled cAMP reached 63% in *M. smegmatis*, 54% in *M. marinum* and 45% in Mtb. Upon exposure to 250 mM NaCl, although the pool size of cAMP decreased in both *M. smegmatis* and Mtb and remained unchanged in *M. marinum* (Fig. 1), the percentage of labelled molecules increased, suggesting an increase in the turn-over of cAMP. Effectively, at 1 doubling time, a 1.3-fold increase in the percentage of labelled cAMP was observed in *M. smegmatis* and 1.8-fold, 1.5-fold and 1.3-fold increases were observed in *M. marinum* at ¼, 1 and 2 doubling times, respectively, compared to non-NaCl-challenged bacteria. Similarly, in Mtb, a 1.8-fold, 1.4-fold and 1.3-fold increase in the percentage of cAMP labelled was observed upon exposure to 250 mM compared to 10 mM at ¼, 1 and 2 doubling times, respectively (Fig. 3C). These data clearly suggest that at a concentration of 250 mM NaCl, in the three species tested in this study, the adenylate cyclases are active, and NaCl seems to promote an increase in their activity despite their biochemical diversity [33], as observed by the augmentation of ^{13}C label incorporated in cAMP over time in *M. smegmatis*, *M. marinum* and Mtb (Fig. 3). Altogether, these data possibly ruled out the hypothesis that in *M. smegmatis* and *M. marinum,* the adenylate cyclases exhibit a reduction in their enzymatic activity to explain the intracellular cAMP levels observed in those species at 250 mM NaCl (Fig. 1). However, compared to *M. smegmatis* and *M. marinum,* even if there is an increase in the turn-over of cAMP of those mycobacterial species, only Mtb is able to increase and maintain higher intracellular cAMP levels upon exposure to 250 mM NaCl.

In summary, experiments using stable isotope labelling coupled to metabolomic analysis revealed the first evidence that mycobacteria are able to adapt their intracellular cAMP levels and turn-over under NaCl stress conditions.

3.3. Increase in intracellular cAMP levels is partially dependent on the PknD osmosensing signalling pathway in Mycobacterium tuberculosis

At this stage, the increase in intracellular cAMP levels found in Mtb could be due to a difference in transcriptome profiles of the enzymes involved in cAMP synthesis and degradation upon exposure to 250 mM NaCl compared to 10 mM NaCl. We therefore used cDNA microarrays to test this hypothesis. cDNA microarray analysis was carried out at

250 mM after 1/12, 1/3 and 1 doubling times. Surprisingly, at 250 mM NaCl, no significant changes in gene expression in genes involved in cAMP synthesis were observed during the measured time course (Supplementary Table S1). This observation is consistent with data from the literature where exposure to 250 mM NaCl for 0.2 doubling time led to minor changes in transcriptome profile in Mtb CDC 1551 [21]. Therefore, we hypothesized that the increase in intracellular cAMP levels observed in Mtb must be driven by a much faster sensing mechanism such as protein phosphorylation cascades. This fast response likely involves pre-existing signal transduction and allosteric regulation of key enzymes and transporters. Eukaryotic-like serine-threonine kinases such as PknD are candidates for orchestrating the early increase in cAMP [22]. Hatzios et al. demonstrated that Mtb uses the eukaryotic-like serine-threonine kinase PknD (Rv0931c) to sense and adapt to NaCl stress [22]. In their report, the authors showed that PknD is one of the first sensors of NaCl stress that dictates the adaptive response via phosphorylation of the anti-sigma factor Rv0516c. To test the hypothesis that PknD is involved in the regulation of the intracellular cAMP levels via phosphorylation of key enzymes involved in cAMP synthesis, the parental strain and a well-characterized *pknD* transposon mutant strain were grown at 10 mM and 250 mM to assess cell viability; these strains were also exposed for ¼ and 1 doubling times to 250 mM NaCl, and their intracellular cAMP levels were measured. As seen in Fig. 4A, at 10 mM NaCl, compared to the parental strain, the *pknD* transposon mutant strain exhibits a defect in growth, which is consistent with the literature [22]. However, when grown in a culture medium containing 250 mM NaCl, the two strains exhibit a similar growth profile (Fig. 4B), even though compared to that under 10 mM NaCl, the growth rate decreases. This observation is surprising since a drastic growth defect in the PknD transposon mutant compared to the parental strain was previously reported [22]. Interestingly, the PknD:Tn strain has 10-fold less intracellular cAMP, with 0.9 ± 0.1 pmoles/100 µg protein, than its parental strain, with 10.4 pmoles/ 100 µg protein (Table 1). This difference could potentially be explained by a decrease in adenylate cyclase activity in the PknD:Tn strain compared to the parental strain in the absence of stress, also explaining the growth defect observed at 10 mM NaCl (Fig. 4A). However, regarding intracellular cAMP levels in those strains (Fig. 4C), exposure to 250 mM NaCl for ¼ and 1 doubling times led to a 3.5-fold and 2.5-fold increase in intracellular cAMP levels, respectively, compared to those in unexposed parental and PknD:Tn strains. After 1 doubling time exposure to 250 mM NaCl, a 2-fold increase in intracellular cAMP levels was observed in both strains. Notably, when exposed for 1 doubling time at 250 mM NaCl, a 3-fold increase in intracellular cAMP levels was observed in Mtb H37Rv, and a 2-fold increase in intracellular cAMP levels was observed in Mtb CDC1551. This difference could potentially be explained by the presence of polymorphic regions in Mtb CDC1551 compared to H37Rv, such as the adenylate cyclases Rv1318c-Rv1320c, which should be further investigated [47]. Overall, at ¼ doubling time, PknD may partly be involved the process of increase in intracellular cAMP levels but not after 1 doubling time, at which levels are similar to those found in the parental strain in the PknD:Tn strain. Therefore, the production of cAMP upon exposure to 250 mM NaCl does not completely follow the classic osmosensory signalling mediated by PknD, suggesting that other partners must be involved in orchestrating the increase in intracellular cAMP levels in Mtb.

3.4. The increase in intracellular cAMP levels is dependent on the transcriptional regulator CRP in Mycobacterium tuberculosis

In *E. coli*, the cAMP receptor protein CRP is involved in transcriptional regulation during NaCl stress [7,8]. To investigate whether CRP plays a role in the upregulation of cAMP under osmotic stress in Mtb, a NaCl stress assay was performed with a Mtb H37Rv strain deleted for the gene *rv3676* (*crp*) and its complemented strain. As previously reported, a growth defect was observed in Mtb lacking *crp* [48,49]. There
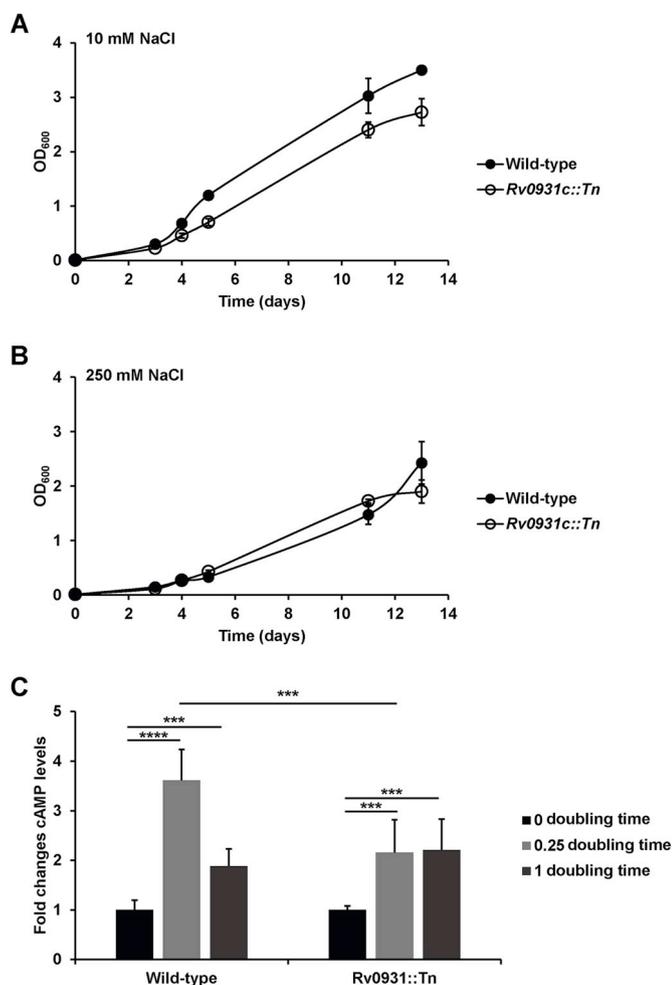
Fig. 4. Effect of NaCl stress on the growth and intracellular cAMP levels of *M. tuberculosis* CDC1551- and PKnD:Tn-deleted strains. Growth curves of parental strain (filled circle) and PKnD:Tn strain (open circle) at 10 mM NaCl (A) and 250 mM NaCl (B) in Middlebrook 7H9 medium monitored at OD 600 nm. (C) Bar graph showing the intracellular levels of cAMP of the parental strain and PKnD:Tn strain. Time 0: black bar; 1/4 doubling time: light grey bar; 1 doubling time: grey bar. Data are the average of two biological replicates and three technical replicates. Data are presented as fold changes corresponding to the ratio of cAMP levels at 250 mM NaCl over cAMP levels at 10 mM NaCl of the corresponding time point.***p < 0.001, ****p < 0.0001 as analysed by Student's *t*-test.

Fig. 5. Effect of NaCl stress on the growth and intracellular cAMP levels of *M. tuberculosis* CRP-deleted strain. Growth curves of Mtb H37Rv wild type (filled circle), MtbΔRv3676 (open circle), and MtbΔRv3676:Rv3676 (filled diamond) at 10 mM NaCl (A) and 250 mM NaCl (B) in Middlebrook 7H9 medium monitored at OD 600 nm. (C) Bar graph showing the intracellular levels of cAMP of the parental strain Mtb H37Rv wild type, MtbΔRv3676, and MtbΔRv3676:Rv3676. Time 0: black bar; 1/4 doubling time: light grey bar; 1 doubling time: grey bar. Data are the average of two biological replicates and three technical replicates. Data are presented as fold changes corresponding to the ratio of cAMP levels at 250 mM NaCl over cAMP levels at 10 mM NaCl of the corresponding time point.*p < 0.05, ***p < 0.001, ****p < 0.0001 as analysed by Student's *t*-test.

is a clear inverse correlation between the concentration of NaCl in the culture medium and the growth kinetics of Mtb [23]. We therefore performed growth curves of Mtb wild type, Δ*crp* and its complemented strain at 10 mM and 250 mM to investigate the impact of NaCl concentrations on growth. Compared to the parental and complemented strains, the Mtb Δ*crp* used here has similar basal intracellular cAMP concentrations of approximately 2 pmoles/100 µg protein (Table 1). As expected, 250 mM NaCl did not abolish the growth of Mtb Δ*crp* but rather slowed the growth of all the strains tested (Fig. 5A and B). We then determined the intracellular cAMP levels in those strains when exposed for 1/4 and 1 doubling times to 250 mM NaCl (Fig. 5C and Table 1). As seen in Fig. 5C, compared to the parental strain, where the intracellular level of cAMP increased by 6-fold after 1/4 doubling time and 3-fold after 1 doubling time exposure to 250 mM NaCl, the strain deleted for *crp* did not exhibit such a drastic increase in the intracellular cAMP levels. Even if the treatment with NaCl could trigger the increase in cAMP in the complemented strain, compared to the parental strain, the complemented strain exhibited higher intracellular cAMP levels after 1 doubling time exposure to a concentration of 250 mM NaCl. This
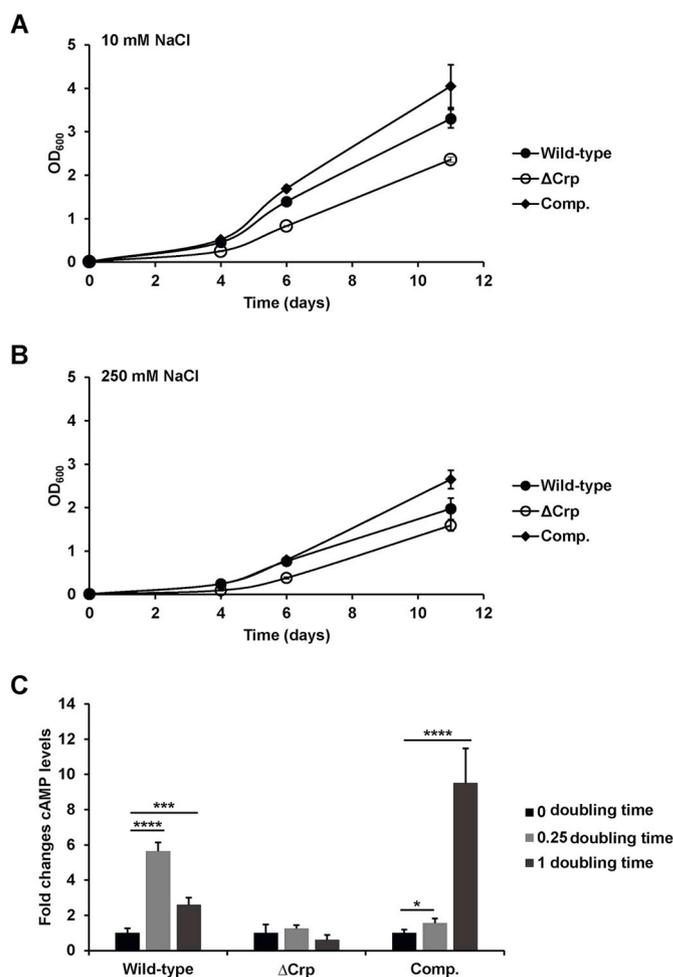
effect might be due to the higher CRP expression in the complemented strain used in this study compared to the parental strain [48]. This experiment clearly demonstrates that CRP is required for the 3-fold increase in cAMP in Mtb.

Strikingly, even though *M. marinum* possesses 31 adenylate cyclases and *M. smegmatis* contains 8 adenylate cyclases as well as the *crp* gene, those species are not able to increase and maintain their intracellular cAMP pool size in response to physiological concentrations of NaCl compared to the response exhibited by Mtb. The complete mechanism remains to be elucidated. However, the first avenue of investigation could be to determine the levels of expression of the adenylate cyclases in Mtb and Δ*crp*. As reported in the literature, compared to the parental strain, the Δ*crp* strain has a 2-fold, 2.7-fold, 1.8-fold and 1.6-fold decrease in Rv3645, Rv1320c, Rv1318c and Rv1625c (cya), respectively, and a 3-fold and 2.6-fold increase in Rv0386 and Rv0891c, respectively [25,45]. Furthermore, we could compare the presence of common and unique adenylate cyclases in *M. smegmatis*, *M. marinum* and Mtb. Rv1359 and Rv2488c are two class III adenylate cyclases found only in

Mtb [33], but as discussed earlier, these enzymes do not exhibit significant changes in transcript levels in the Δ*crp* mutant compared to the parental strain, ruling out a potential involvement of these adenylate cyclases in this process based only on RNASeq data [25].

To decipher the increase in intracellular cAMP levels observed in Mtb, the second hypothesis could be the reduction in the degradation of cAMP by a cyclic-nucleotide phosphodiesterase under exposure to a concentration of 250 mM NaCl in Mtb compared to *M. smegmatis*, *M. marinum* and Mtb Δ*crp*. To date, Rv0805 is the only cAMP phosphodiesterase identified and is found in only slow-growing mycobacteria [50–52]. Interestingly, the *rv0805* gene is proposed to be regulated by CRP [25,53], making Rv0805 a good candidate to explain the phenotype observed in Mtb but not in *M. smegmatis,* in which no homologues have been identified. To support the hypothesis that an alteration of the degradation of cAMP upon exposure to a concentration of 250 mM NaCl occurs, the presence of other cAMP phosphodiesterases in mycobacteria and the modulation of their activity under NaCl stress should be investigated. The identification and characterization of the cAMP phosphodiesterase(s) also still need to be explored.

Nevertheless, to test this hypothesis, we performed ^{13}C stable isotope tracing at ¼ and 1 doubling times (Supplementary Fig. 3). The bacteria were stressed in a culture medium supplemented with either 10 mM or 250 mM NaCl in the presence of [U-^{13}C$_3$] glycerol and [U-^{13}C$_6$] glucose. At 10 mM NaCl, all strains used here exhibited an increase in the percentage of labelled cAMP over time, ruling out non-expression or a lack of activity of the adenylate cyclases in those strains, which is in accordance with the literature. At 250 mM, after ¼ doubling time, the parental strain exhibited a 34% increase in ^{13}C incorporation and the complemented strain a 45% increase compared to that under 10 mM NaCl exposure, which is consistent with the data presented in Figs. 3 and 5C. At 250 mM NaCl, in the Mtb Δ*crp*, this increase was not significant compared to the increase found upon exposure to 10 mM NaCl. Nevertheless, after 1 doubling time under the conditions tested, the percentage of intracellular labelled cAMP reached 40% for all the strains, suggesting that the lack of *crp* does not affect the overall turnover of intracellular levels of cAMP.

Taken together, the findings of this study provide the first evidence that only Mtb is able to increase and maintain its intracellular levels of cAMP in response to NaCl stress and that CRP is necessary in this process. However, the complete and sophisticated mechanism and role of CRP/cAMP still need to be elucidated.

Conflicts of interest

The authors declare that they have no conflicts of interest regarding the content of this article.

Author contribution

SRR and GLM conceived, designed experiments, performed experiments, analysed data, and wrote the paper.

Accession number

cDNA microarray data have been submitted to the Gene Expression Omnibus (GEO) under accession number GSE90839.

Funding

Acknowledgments

Appendix A. Supplementary data

Supplementary data to this article can be found online at https://doi.org/10.1016/j.tube.2019.03.009.

References

[1] Corrigan RM, Grundling A. Cyclic di-AMP: another second messenger enters the fray. Nat Rev Microbiol 2013;11:513–24.

[2] McDonough KA, Rodriguez A. The myriad roles of cyclic AMP in microbial pathogens: from signal to sword. Nat Rev Microbiol 2012;10:27–38.

[3] Dalebroux ZD, Swanson MS. ppGpp: magic beyond RNA polymerase. Nat Rev Microbiol 2012;10:203–12.

[4] Kolb A, Busby S, Buc H, Garges S, Adhya S. Transcriptional regulation by cAMP and its receptor protein. Annu Rev Biochem 1993;62:749–95.

[5] Botsford JL, Harman JG. Cyclic AMP in prokaryotes. Microbiol Rev 1992;56:100–22.

[6] Sevin DC, Sauer U. Ubiquinone accumulation improves osmotic-stress tolerance in Escherichia coli. Nat Chem Biol 2014;10:266–72.

[7] Landis L, Xu J, Johnson RC. The cAMP receptor protein CRP can function as an osmoregulator of transcription in Escherichia coli. Genes Dev 1999;13:3081–91.

[8] Balsalobre C, Johansson J, Uhlin BE. Cyclic AMP-dependent osmoregulation of crp gene expression in Escherichia coli. J Bacteriol 2006;188:5935–44.

[9] Agarwal N, Lamichhane G, Gupta R, Nolan S, Bishai WR. Cyclic AMP intoxication of macrophages by a Mycobacterium tuberculosis adenylate cyclase. Nature 2009;460:98–102.

[10] Agarwal N, Bishai WR. cAMP signaling in Mycobacterium tuberculosis. Indian J Exp Biol 2009;47:393–400.

[11] Nambi S, Basu N, Visweswariah SS. cAMP-regulated protein lysine acetylases in mycobacteria. J Biol Chem 2010;285:24313–23.

[12] Lowrie DB, Jackett PS, Ratcliffe NA. Mycobacterium microti may protect itself from intracellular destruction by releasing cyclic AMP into phagosomes. Nature 1975;254:600–2.

[13] Bai G, Schaak DD, McDonough KA. cAMP levels within Mycobacterium tuberculosis and Mycobacterium bovis BCG increase upon infection of macrophages. FEMS Immunol Med Microbiol 2009;55:68–73.

[14] Roach SK, Lee SB, Schorey JS. Differential activation of the transcription factor cyclic AMP response element binding protein (CREB) in macrophages following infection with pathogenic and nonpathogenic mycobacteria and role for CREB in tumor necrosis factor alpha production. Infect Immun 2005;73:514–22.

[15] Yadav M, Roach SK, Schorey JS. Increased mitogen-activated protein kinase activity and TNF-alpha production associated with Mycobacterium smegmatis- but not Mycobacterium avium-infected macrophages requires prolonged stimulation of the calmodulin/calmodulin kinase and cyclic AMP/protein kinase A pathways. J Immunol 2004;172:5588–97.

[16] Kalamidas SA, Kuehnel MP, Peyron P, Rybin V, Rauch S, Kotoulas OB, Houslay M, Hemmings BA, Gutierrez MG, Anes E, Griffiths G. cAMP synthesis and degradation by phagosomes regulate actin assembly and fusion events: consequences for mycobacteria. J Cell Sci 2006;119:3686–94.

[17] Kaur H, Khuller GK. Role of cyclic adenosine monophosphate in phospholipid synthesis in Mycobacterium smegmatis ATCC 607. Lipids 1995;30:345–9.

[18] Shleeva M, Goncharenko A, Kudykina Y, Young D, Young M, Kaprelyants A. Cyclic amp-dependent resuscitation of dormant mycobacteria by exogenous free Fatty acids. PLoS One 2013;8:e82914.

[19] Dass BK, Sharma R, Shenoy AR, Mattoo R, Visweswariah SS. Cyclic AMP in mycobacteria: characterization and functional role of the Rv1647 ortholog in Mycobacterium smegmatis. J Bacteriol 2008;190:3824–34.

[20] Choudhary E, Bishai W, Agarwal N. Expression of a subset of heat stress induced genes of mycobacterium tuberculosis is regulated by 3',5'-cyclic AMP. PLoS One 2014;9:e89759.

[21] Tan S, Sukumar N, Abramovitch RB, Parish T, Russell DG. Mycobacterium tuberculosis responds to chloride and pH as synergistic cues to the immune status of its host cell. PLoS Pathog 2013;9:e1003282.

[22] Hatzios SK, Baer CE, Rustad TR, Siegrist MS, Pang JM, Ortega C, Alber T, Grundner C, Sherman DR, Bertozzi CR. Osmosensory signaling in Mycobacterium tuberculosis mediated by a eukaryotic-like Ser/Thr protein kinase. Proc Natl Acad Sci U S A 2013;110. E5069-5077.

[23] Larrouy-Maumus G, Marino LB, Madduri AV, Ragan TJ, Hunt DM, Bassano L, Gutierrez MG, Moody DB, Pavan FR, de Carvalho LP. Cell-envelope remodeling as a determinant of phenotypic antibacterial tolerance in Mycobacterium tuberculosis. ACS Infect Dis 2016;2:352–60.

[24] Asmar S, Sassi M, Phelippeau M, Drancourt M. Inverse correlation between salt tolerance and host-adaptation in mycobacteria. BMC Res Notes 2016;9:249.

[25] Kahramanoglou C, Cortes T, Matange N, Hunt DM, Visweswariah SS, Young DB, Buxton RS. Genomic mapping of cAMP receptor protein (CRP Mt) in Mycobacterium tuberculosis: relation to transcriptional start sites and the role of CRPMt as a transcription factor. Nucleic Acids Res 2014;42:8320–9.

[26] Larrouy-Maumus G, Biswas T, Hunt DM, Kelly G, Tsodikov OV, de Carvalho LP. Discovery of a glycerol 3-phosphate phosphatase reveals glycerophospholipid polar head recycling in Mycobacterium tuberculosis. Proc Natl Acad Sci U S A 2013;110:11320–5.

[27] Gouzy A, Larrouy-Maumus G, Bottai D, Levillain F, Dumas A, Wallach JB, Caire-Brandli I, de Chastellier C, Wu TD, Poincloux R, Brosch R, Guerquin-Kern JL, Schnappinger D, Sorio de Carvalho LP, Poquet Y, Neyrolles O. Mycobacterium tuberculosis exploits asparagine to assimilate nitrogen and resist acid stress during infection. PLoS Pathog 2014;10:e1003928.

[28] Gouzy A, Larrouy-Maumus G, Wu TD, Peixoto A, Levillain F, Lugo-Villarino G, Guerquin-Kern JL, de Carvalho LP, Poquet Y, Neyrolles O. Mycobacterium tuberculosis nitrogen assimilation and host colonization require aspartate. Nat Chem Biol 2013;9:674–6.

[29] Nandakumar M, Prosser GA, de Carvalho LP, Rhee K. Metabolomics of Mycobacterium tuberculosis. Methods Mol Biol 2015;1285:105–15.

[30] de Carvalho LP, Fischer SM, Marrero J, Nathan C, Ehrt S, Rhee KY. Metabolomics of Mycobacterium tuberculosis reveals compartmentalized co-catabolism of carbon substrates. Chem Biol 2010;17:1122–31.

[31] Holmes DT, Buhr KA. Error propagation in calculated ratios. Clin Biochem 2007;40:728–34.

[32] Padh H, Venkitasubramanian TA. Adenosine 3',5'-monophosphate in Mycobacterium phlei and Mycobacterium tuberculosis H37Ra. Microbios 1976;16:183–9.

[33] Shenoy AR, Visweswariah SS. Mycobacterial adenylyl cyclases: biochemical diversity and structural plasticity. FEBS Lett 2006;580:3344–52.

[34] Casey SJ, Ford MJ, Gazdik MA. The role of transcriptional regulation in maintaining the availability of mycobacterial adenylate cyclases. PeerJ 2014;2:e298.

[35] McCue LA, McDonough KA, Lawrence CE. Functional classification of cNMP-binding proteins and nucleotide cyclases with implications for novel regulatory pathways in Mycobacterium tuberculosis. Genome Res 2000;10:204–19.

[36] Gazdik MA, Bai G, Wu Y, McDonough KA. Rv1675c (cmr) regulates intramacrophage and cyclic AMP-induced gene expression in Mycobacterium tuberculosis-complex mycobacteria. Mol Microbiol 2009;71:434–48.

[37] Stapleton M, Haq I, Hunt DM, Arnvig KB, Artymiuk PJ, Buxton RS, Green J. Mycobacterium tuberculosis cAMP receptor protein (Rv3676) differs from the Escherichia coli paradigm in its cAMP binding and DNA binding properties and transcription activation properties. J Biol Chem 2010;285:7016–27.

[38] Nambi S, Gupta K, Bhattacharyya M, Ramakrishnan P, Ravikumar V, Siddiqui N, Thomas AT, Visweswariah SS. Cyclic AMP-dependent protein lysine acylation in mycobacteria regulates fatty acid and propionate metabolism. J Biol Chem 2013;288:14114–24.

[39] Nambi S, Badireddy S, Visweswariah SS, Anand GS. Cyclic AMP-induced conformational changes in mycobacterial protein acetyltransferases. J Biol Chem 2012;287:18115–29.

[40] Ott A, Oehme F, Keller H, Schuster SC. Osmotic stress response in Dictyostelium is mediated by cAMP. EMBO J 2000;19:5782–92.

[41] Imashimizu M, Yoshimura H, Katoh H, Ehira S, Ohmori M. NaCl enhances cellular cAMP and upregulates genes related to heterocyst development in the cyanobacterium, Anabaena sp. strain PCC 7120. FEMS Microbiol Lett 2005;252:97–103.

[42] Jackson EK. The 2',3'-cAMP-adenosine pathway. Am J Physiol Renal Physiol 2011;301:F1160–7.

[43] Li X, Mei H, Chen F, Tang Q, Yu Z, Cao X, Andongma BT, Chou SH, He J. Transcriptome landscape of Mycobacterium smegmatis. Front Microbiol 2017;8:2505.

[44] Wang S, Dong X, Zhu Y, Wang C, Sun G, Luo T, Tian W, Zheng H, Gao Q. Revealing of Mycobacterium marinum transcriptome by RNA-seq. PLoS One 2013;8:e75828.

[45] Cortes T, Schubert OT, Rose G, Arnvig KB, Comas I, Aebersold R, Young DB. Genome-wide mapping of transcriptional start sites defines an extensive leaderless transcriptome in Mycobacterium tuberculosis. Cell Rep 2013;5:1121–31.

[46] Shenoy AR, Sivakumar K, Krupa A, Srinivasan N, Visweswariah SS. A survey of nucleotide cyclases in actinobacteria: unique domain organization and expansion of the class III cyclase family in Mycobacterium tuberculosis. Comp Funct Genom 2004;5:17–38.

[47] Fleischmann RD, Alland D, Eisen JA, Carpenter L, White O, Peterson J, DeBoy R, Dodson R, Gwinn M, Haft D, Hickey E, Kolonay JF, Nelson WC, Umayam LA, Ermolaeva M, Salzberg SL, Delcher A, Utterback T, Weidman J, Khouri H, Gill J, Mikula A, Bishai W, Jacobs Jr. WR, Venter JC, Fraser CM. Whole-genome comparison of Mycobacterium tuberculosis clinical and laboratory strains. J Bacteriol 2002;184:5479–90.

[48] Rickman L, Scott C, Hunt DM, Hutchinson T, Menendez MC, Whalan R, Hinds J, Colston MJ, Green J, Buxton RS. A member of the cAMP receptor protein family of transcription regulators in Mycobacterium tuberculosis is required for virulence in mice and controls transcription of the rpfA gene coding for a resuscitation promoting factor. Mol Microbiol 2005;56:1274–86.

[49] Bai G, Schaak DD, Smith EA, McDonough KA. Dysregulation of serine biosynthesis contributes to the growth defect of a Mycobacterium tuberculosis crp mutant. Mol Microbiol 2011;82:180–98.

[50] Matange N. Revisiting bacterial cyclic nucleotide phosphodiesterases: cyclic AMP hydrolysis and beyond. FEMS Microbiol Lett 2015;**362**.

[51] Matange N, Hunt DM, Buxton RS, Visweswariah SS. Overexpression of the Rv0805 phosphodiesterase elicits a cAMP-independent transcriptional response. Tuberculosis 2013;93:492–500.

[52] Shenoy AR, Sreenath N, Podobnik M, Kovacevic M, Visweswariah SS. The Rv0805 gene from Mycobacterium tuberculosis encodes a 3',5'-cyclic nucleotide phosphodiesterase: biochemical and mutational analysis. Biochemistry 2005;44:15695–704.

[53] Bai G, McCue LA, McDonough KA. Characterization of Mycobacterium tuberculosis Rv3676 (CRPMt), a cyclic AMP receptor protein-like DNA binding protein. J Bacteriol 2005;187:7795–804.